



Inferring resource distributions from Atlantic bluefin tuna movements: An analysis based on net displacement and length of track

Ryan Gutenkunst^{a,*}, Nathaniel Newlands^b, Molly Lutcavage^c, Leah Edelstein-Keshet^d

^aLaboratory of Atomic and Solid State Physics, Cornell University, Ithaca, NY 14853-2501, USA

^bAgriculture and Agri-Food Canada Research Centre, 5403 1st Avenue S., P.O. Box 3000, Lethbridge, AB, Canada T1J 4B1

^cDepartment of Zoology, University of New Hampshire, Durham, NH 03824-2617, USA

^dDepartment of Mathematics, University of British Columbia, Vancouver, BC, Canada V6T 1Z2

Received 11 April 2006; received in revised form 27 September 2006; accepted 16 October 2006

Abstract

We use observed movement tracks of Atlantic bluefin tuna in the Gulf of Maine and mathematical modeling of this movement to identify possible resource patches. We infer bounds on the overall sizes and distribution of such patches, even though they are difficult to quantify by direct observation *in situ*. To do so, we segment individual fish tracks into intervals of distinct motion types based on the ratio of net displacement to length of track ($\Delta D/\Delta L$) over a time window Δt . To find the best segmentation, we optimize the fit of a random-walk movement model to each motion type. We compare results from two distinct movement models: biased turning and biased speed, to check the model-dependence of our inferences, and find that uncertainty in choice of movement model dominates the uncertainties of our conclusions. We find that our data are best described using two motion types: “localized” ($\Delta D/\Delta L$ small) and “long-ranged” ($\Delta D/\Delta L$ large). The biased turning model leads to significantly better resolution of localized movement intervals than the biased speed model. We hypothesize that localized movement corresponds to exploitation of resource patches. Comparison with visual behavior observations made during tracking suggests that many inferred intervals of localized motion do indeed correspond to feeding activity. From our analysis, we estimate that, on average, bluefin tuna in the Gulf of Maine encounter a resource patch every 2 h, that those patches have an average radius of 0.7–1.2 km, and that, overall, there are at most 5–9 such patches per 100 km² in the region studied. © 2006 Elsevier Ltd. All rights reserved.

Keywords: Atlantic bluefin tuna; Resource patch distribution; Localized and long-ranged motion; Correlated biased random walk

Over the last decade, populations of major fish stocks worldwide have dwindled to near collapse (Pauly et al., 1998). Conservation efforts mandate a fuller understanding of the foraging, navigating, and migrating behavior of economically important fish such as Atlantic bluefin tuna (*Thunnus thynnus* L.), the subject of this paper. A number of groups have worked on collecting (Block et al., 2005) and/or analyzing (Sibert et al., 2003; Royer et al., 2005; Wilson et al., 2005; Sibert et al., 2006) tuna movement data. Recent observations demonstrate that tuna school positions are correlated with oceanic fronts and thermal features (Schick

et al., 2004). However, not all aspects of tuna school distributions and movement patterns can be explained by such features (Royer et al., 2004); there is a tendency to over-aggregate at small scales and over-disperse at larger scales. Some aspects are likely due to intra- and inter-species interactions, particularly with prey, which are often patchily distributed (Chase, 2002). How bluefin tuna navigate to find resources is not well understood, in part because quantitative data on movement, environment, and prey have not been collected concurrently (Kirby, 2001; Newlands and Lutcavage, 2001). Here we use a statistical and modeling approach to draw inferences from a limited number of detailed bluefin tuna trajectories about the unknown distribution of resources they utilize in the Gulf of Maine.

In many previous animal track analyses, resource sites were a priori identifiable, and movement behavior could

*Corresponding author. Tel.: +1 607 255 6068; fax: +1 607 255 6428.

E-mail addresses: rng7@cornell.edu (R. Gutenkunst), newlandsn@agr.gc.ca (N. Newlands), molly.lutcavage@unh.edu (M. Lutcavage), keshet@math.ubc.ca (L. Edelstein-Keshet).

then be directly correlated to such features. For example, Ward and Saltz (1994) relate gazelle foraging tracks to observed clusters of lilies in the sands of the Negev desert. In our work, we do not assume any a priori environmental information, but rather, we ask what can be inferred directly from track data; where and how long did individuals linger, and how large and closely spaced were such “sites”? In many previous treatments of animal and fish movements, the main goals have been (a) to use observations and models at the individual level to derive population dispersal parameters (Grünbaum, 1994, 1998, 1999), (b) to use trajectories to infer the mechanisms that animals use to navigate, e.g. by taxis or klinokinesis (Benhamou and Bovet, 1992), or (c) to compare measures such as displacement and mean squared displacement to those predicted by traditional random and correlated or biased random walk models. We are not aware of studies that ask how information about resource patches can be gleaned from movement paths of tuna, but a related study on dolphins with distinct methodology has recently appeared (Bailey and Thompson, 2006, reviewed in the Discussion). The use of large-scale tracks to draw environmental inferences is the significantly new aspect of our study on tuna in this paper.

We analyse movement of bluefin tuna using data from the Gulf of Maine (Fig. 1). Some of this data has been presented (Lutcavage et al., 2000) and analysed (Newlands and Lutcavage, 2001) before, but with different aims (reviewed in the Discussion). For example, Newlands et al.

(2004) looked for correlations between speed and rates of turning along the tracks.

Here we concentrate on horizontal movement of individuals. The vertical components of these trajectories are on a much smaller spatial scale (Lutcavage et al., 2000) and are here ignored. Even simple visual inspection reveals that some tracks (e.g. labeled 9602 in Fig. 1, and also shown enlarged in Fig. 5) have relatively straight, long-ranged portions (eastern portion), interspersed with convoluted localized segments (western portion). This observation motivated our identification of distinct motion types as localized versus long-ranged and informed our choice of criterion for classifying such movements. However, as seen from other tracks (e.g. 9604a in Fig. 1, and enlarged in Fig. 6), visual inspection is not always acute or objective enough to easily decompose a track into these two categories. This led to our quantitative analysis and our selection of an objective criterion to classify track portions.

Our idea is to associate putative resource patches with localized segments of track data, and time spent searching for resources with long-ranged segments. In the following sections, we describe the data, how we picked a criterion for segmentation, and how we determined the optimal segmentation. Our segmentation optimization depends on a movement model, and we describe and evaluate two movement models. We find that our results on time spent searching for resources are relatively insensitive to model choice, but our estimates of the size of resource patches are sensitive to model choice. We then present estimates for the

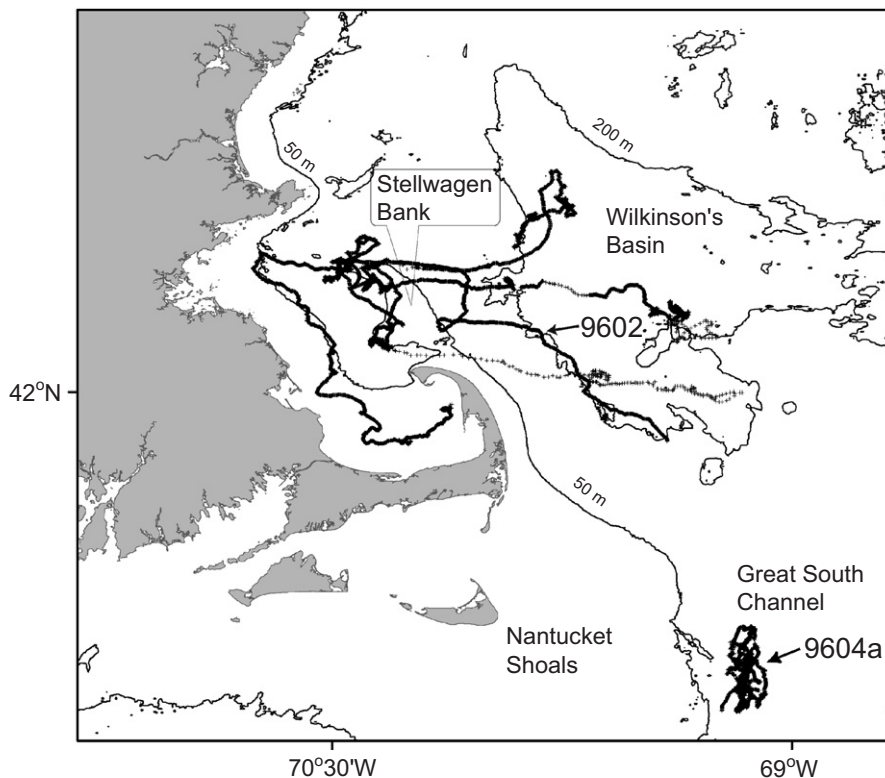


Fig. 1. Gulf of Maine showing data points for recorded tracks of Atlantic bluefin tuna considered in this study (small crosses) and bathymetry of the Gulf (thin curves). Tracks labeled 9602 and 9604a appear in Figs. 5 and 6.

distribution of resource patches that bluefin tuna utilize in the Gulf of Maine. In absence of other data, these could serve as initial estimates for concentrations of prey or other resources.

1. Data

Our bluefin tuna movement data consist of 12 detailed tracks recorded between 1995 and 1997 at several locations within the Gulf of Maine. (Fig. 1 and Table 1; see also Lutcavage et al., 2000). Each track is an independent record of the positions of an individual adult bluefin tuna (swimming within its school), tracked by boat with acoustic transmitters to a resolution of a few meters for up to 48 h. For most tracks, the median time between position recordings was 1 min, and one track (9603) sampled at a higher rate was down-sampled to this rate. Some tracks contained gaps of up to 1 h (Table 1). We interpolated over such gaps with straight-line motion. (Gaps longer than 15 min did not comprise more than 6% of the total duration of any track.) It is estimated that the measurement error (on the order of 10 m) is approximately constant across and between tracks. As the tracks each span tens of kilometers, this error is small relative to distance scales of interest in this study. Anecdotal information on tidal and prey activity was also compiled, and we compare our results with these observations in the Discussion section. Vertical motions of the tuna were generally restricted to a few tens of meters of the sea surface while horizontal motions extended over tens of kilometers (Lutcavage et al., 2000).

In Fig. 1, bluefin tuna tracks comprising our data set are shown superimposed on a map of the Gulf of Maine. The data give strong evidence of long-ranged, directionally persistent motion (Fig. 1). Though tracks were followed on separate days and for distinct individuals, on a global scale of many tens and up to hundreds of kilometers, these tracks are roughly aligned with each other and with coarse features of the bathymetry. For example, several of the bluefin tuna lingered near Stellwagen Bank, and two

individuals seem to track the edge of Wilkinson's Basin. This correlation between movement and bathymetry motivated the inclusion of bias in the random-walk movement models we chose to test.

2. Methods

2.1. Data segmentation

For any two times, t_1 and t_2 , and positions along the track, $\vec{x}_1 = \vec{x}(t_1)$ and $\vec{x}_2 = \vec{x}(t_2)$ at those times, we define the net displacement $D(t_1, t_2)$ as the straight line distance between \vec{x}_1 and \vec{x}_2 , and the track length $L(t_1, t_2)$ as the total (arc) length of track between \vec{x}_1 and \vec{x}_2 . Then for a given time interval Δt ,

$$\Delta D \equiv D(t, t + \Delta t) = |\vec{x}(t + \Delta t) - \vec{x}(t)|,$$

$$\Delta L \equiv L(t, t + \Delta t) = \sum_{t_i \in (t, t + \Delta t)} |\vec{x}(t_{i+1}) - \vec{x}(t_i)|. \quad (1)$$

We occasionally use simply $L(t)$ to refer to total length of track from $t = 0$ to time t .

On a graph of $L(t)$ (e.g. gray curve in Fig. 2) the slope, which is the fish's swimming speed, was nearly constant across tracks and time, despite the fact that observations spanned roughly two days per track. We observe, however, distinct trends in the displacement data, namely portions of the trajectories in which displacement mirrored track length and portions in which displacement changed very little. (See solid and dashed black curves in Fig. 2.) This motivates us to segment the data based on the dimensionless ratio of net displacement to net track length $\Delta D/\Delta L$ over the time window Δt (in min).

Fig. 3 shows a flow-chart summarizing our method. We calculate the increment in the displacement ΔD and the increment in track arc length ΔL from the linearly interpolated track over a time window of duration Δt (min) centered about the midpoint of each step. The resulting time series of $\Delta D/\Delta L$ is smoothed by taking the Fourier transform of its linear interpolation and discarding terms with period less than Δt . Steps are then classified into

Table 1
Track statistics

ID	Duration (h)	Sample interval (s)	Gaps (min)	Length (km)	Displacement (km)
9501	8	300		56	13
9601	29	600	18	136	73
9602	47	60		283	107
9603	8	13	16	176	1
9604a	46	61	18, 26, 27	221	16
9604b	22	61	17, 53	141	6
9605	24	60	16, 17, 53	130	6
9701	47	61	20, 20, 27, 30	239	79
9702	31	61		156	66
9703	6	61		26	15
9704	3	61		21	3
9705	47	61	19, 37, 62, 71	261	39

Tabulated are statistics for the 12 bluefin tuna tracks considered in this study. The listed gaps are all those longer than 15 min.

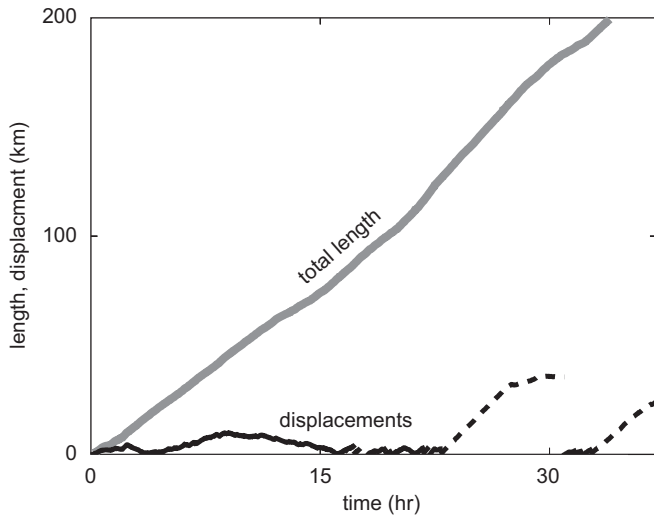


Fig. 2. Comparison of track length, L (km), and net displacement, D (km), as functions of time t (h) from an initial time point. The gray curve shows total track length as a function of time (h) for the portion of track 9602 shown in Fig. 5. Its slope, the swimming speed, is almost constant. The dark (solid and dashed) curves show net displacements from the initial point of each segment in our optimal segmentation, using the biased speed movement model. Solid lines are segments of localized movement, for which net displacement changes slowly relative to track length. Dashed lines are long-ranged segments, for which net displacement is nearly proportional to track length.

motion types based on their ratio $\Delta D/\Delta L$ over the time increment Δt . We term an interval of continuous movement in one type of motion a “segment”.

Most of our analysis presumes two motion types ($\Delta D/\Delta L \leq r$ and $\Delta D/\Delta L > r$), but as a check we also considered the possibility of three types ($\Delta D/\Delta L \leq r_1$, $r_1 < \Delta D/\Delta L \leq r_2$, and $\Delta D/\Delta L > r_2$). The segmentation of the data depends on the time window Δt , and the threshold(s), r (or r_1 and r_2). To select these parameters objectively, we iteratively search through many choices of the segmentation parameters to find the optimal set. To quantify the quality of a segmentation, we fit a movement model to the data for each motion type, as described below. Better segmentations result in better model fits because they more cleanly separate the movement types. When considering two motion types, optimal segmentation parameters are found by searching over the region: $r \in (0.45, 0.90)$, $\Delta t \in (30, 90)$ minutes. Segmentation parameters outside this range yield qualitatively poor results. Similarly, when using three motion types, the region $r_1 \in (0.2, 0.90)$, $r_2 \in (r_1, 0.90)$, $\Delta t \in (30, 90)$ minutes is searched.

2.2. Movement models tested

Our segmentations are scored by how well a model can fit the movements in each motion type. When comparing our model results and data we consider, for each step i , the speed s_i , heading angle θ_i , and turning angle $\phi_i = \theta_i - \theta_{i-1}$, defined in Fig. 4. We also consider the angle between the

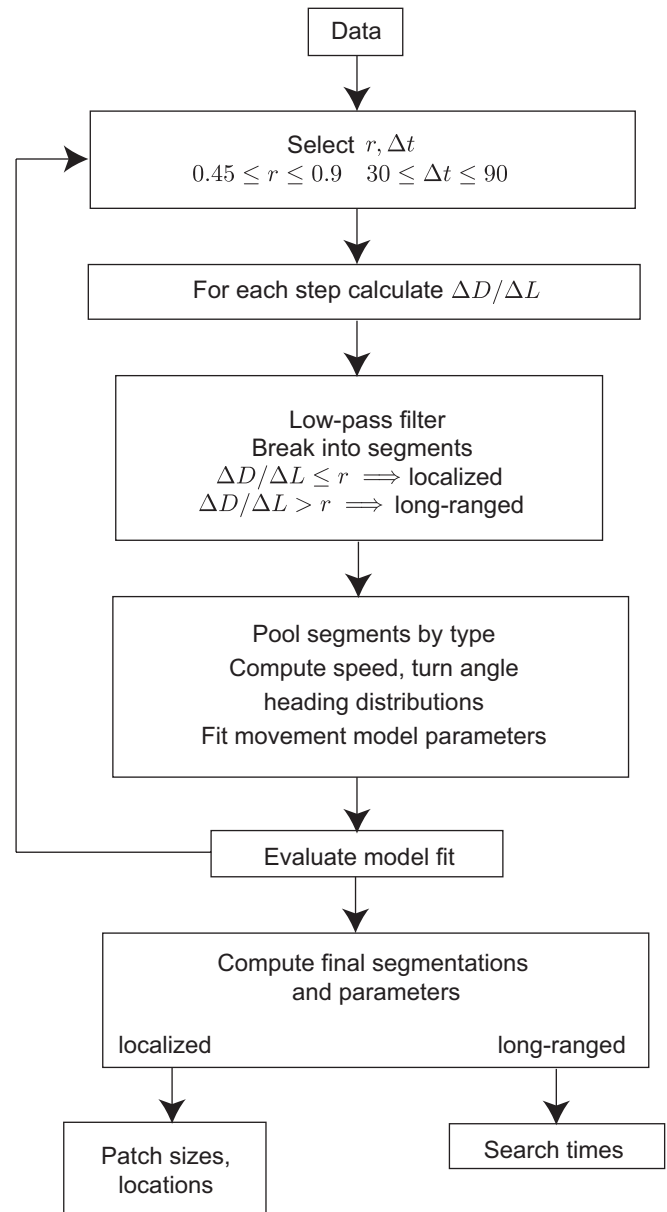


Fig. 3. Illustration of the segmentation and modeling process. For each set of thresholds r on the dimensionless ratio $\Delta D/\Delta L$ and for each time window size Δt (in min), the tracks are segmented and a movement model fit. The fit of that model is used to score the segmentation. Inferences about the environment can be made once the optimal segmentation has been found.

current heading and the “preferred direction”, $\Delta\theta_i = \theta_i - \theta_p$. The preferred direction θ_p is approximated separately for each track segment as an average heading over the complete segment: $\tan \theta_p \equiv \langle \sin \theta \rangle / \langle \cos \theta \rangle$.

To test the sensitivity of our results to the assumptions about bluefin tuna movement encoded by the model chosen, we compare results between two biased random-walk movement models. The details of how tuna navigate and find their way are still uncertain, so this comparison of two distinct models helps to put the results into a broader context. In the first, we assume that turning is biased toward a preferred direction, and in the second, we assume

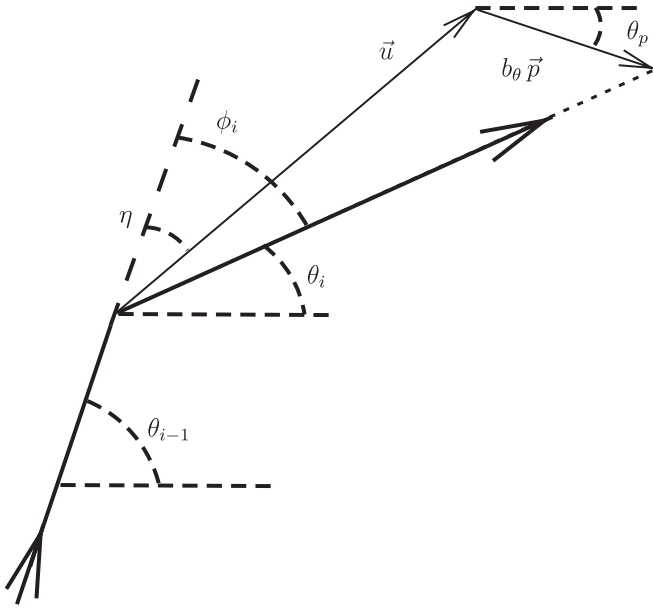


Fig. 4. Notation for the biased turning model. θ_i is the heading angle in step i , i.e. the direction with respect to some arbitrary fixed coordinate system. In the biased turning movement model, a prospective turn angle, η , is chosen from a distribution. The new unit heading vector \vec{u} is then further modified to include bias toward the preferred heading angle θ_p : a vector of length b_θ pointing along \vec{p} is added to \vec{u} to obtain the actual new heading, $\vec{u} + b_\theta \vec{p}$.

that movement speed is biased according to the direction of movement. Both models allow for bias in all motion types to account for possible correlations with ocean features (Newlands and Lutcavage, 2001; Schick et al., 2004).

2.2.1. Biased turning model

In this model, tuna movement is biased in a specific direction by changes in turning angle, which is composed of a random component plus a deterministic bias component. This model is similar to the tactic model with persistence considered by Benhamou and Bovet (1992). They, however, apply bias by shifting the mean of the turn distribution from which a random turn is drawn.

Our model is illustrated in Fig. 4. For each turn, an initial turn angle is randomly drawn from a distribution with zero mean. The unit vector in the resulting heading direction is denoted \vec{u} , and the final heading is found by adding a vectorial bias in the preferred direction. This yields a heading of $\vec{u} + b_\theta \vec{p}$, where \vec{p} is a unit vector in the preferred direction (determined from θ_p as described in the previous section) and b_θ is a dimensionless bias factor.

After experimenting with a variety of commonly used turn angle distributions, we found that the best fit to the data was obtained using a wrapped Laplace distribution (Jammalamadaka and Kozubowski, 2004) for the random component of the turns. For this distribution, the probability $\Pr(\eta)$ of making a turn η falls exponentially with angular range a :

$$\Pr(\eta) \propto \exp(-|\eta|/a), \quad -\pi < \eta \leq \pi.$$

The magnitude of the bias toward the preferred direction b_θ and the angular range a are chosen for each movement type by maximizing the likelihood of the observed heading angle deviation and turn angle distributions. Model heading and turn angle distributions are calculated numerically as described in Appendix A.

The speed of each step is drawn from a Gamma distribution, the most common assumption for such distributions:

$$\Pr(s) \propto s^{k-1} e^{-s/\Sigma},$$

where k and Σ are fit separately for each motion type by maximum likelihood.

To objectively score the segmentation parameters r and Δt when using this movement model, we use the prediction root mean squared error (PRMSE) (Chatfield, 2001). For each step in the data, we calculate the mean next step predicted by the model based on the deviation of the data's current heading from the segment's preferred heading and the segment's current motion type. The PRMSE² is an average over steps of the squared difference between predicted and actual steps:

$$\text{PRMSE}^2 = \frac{1}{N_{\text{steps}}} \sum_{\text{steps}} ((x_{\text{pred}}|\theta_{\text{data}}) - x_{\text{data}})^2 + ((y_{\text{pred}}|\theta_{\text{data}}) - y_{\text{data}})^2. \quad (2)$$

We use this scoring function for the biased turning model because it uses only the means of the model distributions; the full distributions are computationally prohibitive to calculate for each possible heading angle deviation.

2.2.2. Biased speed model

In this model we assume that tuna movement is biased by changes in speed, not turning. As seen in Fig. 2 the variation in swimming speed is small, so we expect this model to fit less well than the biased turning model. We explore this model to gauge how much our conclusions depend on the choice of movement model.

Here, for step i , the speed is chosen from a Gamma distribution whose scale parameter Σ is a function of the current heading angle θ_i . For the dependence of Σ on θ we adopt the functional form:

$$\Sigma(\theta) = \Sigma_0 + b_s \Sigma_0 \exp((1/\sigma_s) \cos(\theta - \theta_p)).$$

The magnitude of the bias is controlled by b_s . For positive b_s , Σ is larger when the heading of the fish is closer to the preferred heading, so, on average, speeds will be higher and steps longer in the preferred direction, biasing the overall motion. To fit the parameters Σ_0 , b_s , and σ_s for each motion type, the steps are divided evenly into 20 bins based on their heading angle deviations. The speeds of the steps in each bin are fit to a Gamma distribution and the resulting values of Σ fit to the above form. The shape parameter k for each motion type is set to the median of the binned values, as we observe no systematic variation in k .

Turns are drawn from a circular Laplace distribution as in the biased turning model, but no bias is applied to turning in this case.

For this model, calculating the full distribution of turns and speeds for a given heading angle deviation is straightforward, so we optimize the segmentation parameters by maximizing the log-likelihood function rather than the PRSME:

$$LL = \sum_{\substack{\text{turns} \\ \text{in data}}} \log \Pr(\phi | \text{motion type}) + \sum_{\substack{\text{steps} \\ \text{in data}}} \log \Pr(s | \theta - \theta_p, \text{motion type}). \quad (3)$$

In Eq. (3) the probability of generating the observed turn ϕ from the model, given the motion type assigned to that turn by the segmentation, is denoted $\Pr(\phi | \text{motion type})$. Similarly, $\Pr(s | \theta - \theta_p, \text{motion type})$ is the probability of generating the observed speed s given the difference between the current and preferred headings and the assigned motion type.

2.3. Inferences about the resource distribution

From the optimal set of segmentation parameters using two motion types, r and Δt , we calculate a final segmentation and set of movement statistics. Segments with $\Delta D / \Delta L \leq r$ are deemed “localized” versus segments with $\Delta D / \Delta L > r$ that are taken to be “long-ranged”. We make inferences about the environment from the properties of these segments.

In particular, we suspect that localized movement corresponds to exploitation of resources. If we make the simple approximation that resources are organized into circular patches, we can estimate the extent of a given patch by the minimal circle required to enclose one full segment of localized motion. The assumption of circularity may overestimate the actual patch size, but the assumption that tuna cease localized motion only upon leaving a patch may lead to an underestimation of patch size.

The transit time between patch encounters can be estimated from the duration of long-ranged movement segments. Given the average patch radius and time between encounters, we can estimate an upper bound on the spatial number density of patches. Each patch presents an average cross-section of $2r_p$ (the patch diameter) to a fish moving toward it. Given ρ randomly distributed patches per unit area, randomly moving tuna must move an average linear distance $1/(2\langle r_p \rangle \rho)$ between patch encounters. Thus, the mean time between patch encounters is $\tau \approx 1/(2\langle r_p \rangle \langle s \rangle \rho)$, where $\langle s \rangle$ is the average velocity component of the tuna along its preferred heading direction. We can estimate $\langle s \rangle$ as the product of the mean step speed and the mean cosine of the angle between the heading and the preferred direction. τ is simply the mean duration of long-ranged motion, and $\langle r_p \rangle$ is obtained from the radii of the enclosing circles described earlier. Real tuna no doubt use environ-

ment cues to more efficiently find resource patches and encounter resources more often than they would if moving randomly, so our estimates of patch number density are upper bounds.

3. Results

Results from the optimal segmentations for both movement models considered are summarized in Table 2. For both movement models we find that the segmentation with two modes performs noticeably better than with one mode. Additionally, for both movement models a three-mode segmentation performed no better than the two-mode segmentation (data not shown). Results for each individual track in our sample are found in the online Supplementary Material.

Examples of tracks optimally segmented using the two movement models are shown in Figs. 5 and 6. Segmentations for all tracks are included in the online Supplementary Material. Fig. 7 shows the segmentation for each track as a function of time.

The distributions of long-range segment durations and localized segment enclosing radii are shown for the optimal segmentations in Fig. 8. The mean duration of long-ranged segments is 2 h using either movement model (Table 2). The patches identified using the biased turning model have a smaller average size than those identified using the biased speed model. In long-ranged motion, the mean cosine of the angle between the heading and the preferred direction is 0.7 in the optimal segmentation using either movement model, and the mean speed projected along the preferred direction is $\langle s \rangle \approx 4$ km/h. The difference in estimated patch number density is thus entirely due to the difference in estimated patch sizes.

Our estimates for the median radius of patches are more sensitive to the choice of the cutoff r than the window size Δt . For either optimal segmentation, an increase in r by 5% yields about a 10% increase in the median radius of patches, while an increase in Δt by 5% yields a 5% increase in the median radius. The mean time spent in long-ranged motion is less sensitive to the segmentation parameters. For either segmentation, an increase in r by 5% yields about a 3% decrease in the mean duration of long-ranged segments, while an increase in Δt by 5% yields a 3% increase in the mean duration.

4. Discussion

4.1. Number of motion types

Our results provide evidence for two distinct types of motion in bluefin tuna. Given either biased turning or biased speed movement model, the model with two movement types fits better than the model with one, and the model with three movement types fits no better than the model with two. This finding is related to similar conclusions of Morales et al. (2004) who modeled elk

Table 2

Optimal segmentation parameters and movement model parameters for the two models (biased turning and biased speed) considered

Biased turning model

Optimal segmentation parameters		Optimal PRSME	Single-mode PRMSE
$r = 0.57$ $\Delta t = 43$ min		129 m	155 m
Motion type	Turning parameters	Speed parameters	Mean speed
Localized	$a = 0.63$ $b_\theta = 0.06$	$k = 3.4$ $\Sigma = 0.5$ m/s	1.61 m/s
Long-range	$a = 0.65$ $b_\theta = 0.56$	$k = 2.3$ $\Sigma = 0.7$ m/s	1.67 m/s
Median localized segment radius	Percent time in localized motion	Mean long-ranged segment duration	Patch number density
0.7 km	30%	2 h	9/100 km ²

Biased speed model

Optimal segmentation parameters		Optimal LL	Single-mode LL
$r = 0.66$ $\Delta t = 60$ min		1.11	1.16
Motion type	Turning parameters	Speed parameters	Mean speed
Localized	$a = 0.64$	$k = 3.7, \Sigma_0 = 0.47$ m/s $b_s = 0.1, \sigma_s = 2.0$	1.60 m/s
Long-range	$a = 0.38$	$k = 2.9, \Sigma_0 = 0.6$ m/s $b_s = 0.25, \sigma_s = 0.6$	1.71 m/s
Median patch radius	Percent time in localized motion	Mean long-ranged segment duration	Patch number density
1.2 km	45%	2 h	5/100 km ²

movements as mixtures of different motion types and found that two types sufficed to explain the data well.

4.2. Comparison of results between the two movement models

The optimal segmentations that we found from the two movement models have similar distributions of long-range segment durations, but the biased turning model yields significantly better resolution of patches than the biased speed model. From Figs. 5–7 it is apparent that large patches found using the biased speed model are broken into clusters of smaller patches if the biased turning model is used instead.

Comparing biases found using the two movement models we find that biases in turning are greater than biases in swimming speeds. (The long-ranged motion bias parameter is larger in the biased turning model, $b_\theta = 0.56$, than in the biased speed model, $b_s = 0.25$.) This suggests that biases in turning are more important for bluefin tuna behavior and implies that the biased turning model represents long-ranged swimming behaviors more faithfully than the biased speed model. The higher quality of the

biased turning fit allows the corresponding segmentation to identify patches with higher resolution.

The sensitivity of the median patch radius to the segmentation parameters is small compared to the difference in median radius between the two movement models. This suggests that the difference is not due to a failure to converge on the optimum segmentation parameters for either model, but is instead due to the inherent difference in assumptions made by the two movement models. These sensitivity results suggest that the dominant uncertainty in our analysis comes from our ignorance of the perfect movement model. Work on developing more complete and realistic movement models will thus play an important role in refining estimates of environmental parameters derived from track data.

4.3. Comparison with observed feeding activity

Prey density was not quantitatively measured while the tuna were tracked, but approximate times of observed feeding activity were recorded (Lutcavage et al., 2000). We can compare our periods of inferred localized motion (Fig. 7) to these observations to test (1) whether localized

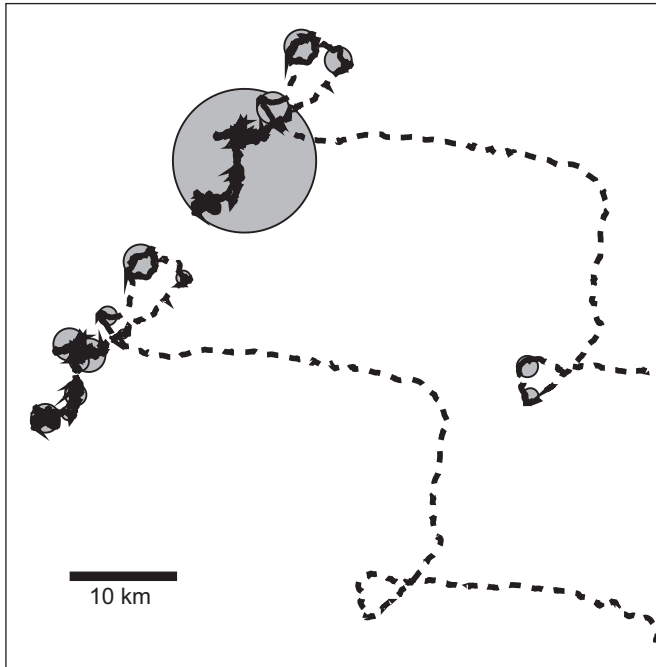


Fig. 5. Portion of a bluefin tuna track (approximately 35 h) showing clear separation between localized and long-ranged movement. This tuna was moving west to east in the Gulf of Maine. The track is drawn twice to illustrate the different segmentation results given the two movement models we consider. Upper copy: biased speed model (tuna adjust their speeds to maintain a heading bias). Lower copy: biased turning model (turning is adjusted to maintain the heading bias.) In both cases, identified localized motion is shown by solid lines and identified long-ranged motion by dashed lines. The gray disks are minimal circles enclosing each localized segment. We hypothesize that these regions correspond to resource patches.

motion corresponds to resource exploitation and (2) whether our algorithm successfully identifies periods of resource exploitation. Below we compare all the observed feeding events with the movement type inferred in our track analysis.

Fish 9501 was observed for 8 h, during which its school fed at the surface. Our analysis identified only a few short intervals of localized motion in 9501's track. Fish 9601 was tracked for 29 h and was seen to feed on sand lance during the afternoon of the second day. Our analysis, however, found very little localized motion in 9601's track, and almost none during the time it was seen feeding. In both these cases our algorithm seems to have performed poorly, identifying as long-ranged periods where the fish were known to be feeding. However, both tracks 9501 and 9601 were sampled at a much lower rate (once every 5 and 10 min, respectively) than the rest of the tracks, which were sampled at least once per minute.

Fish 9602 fed during the afternoon of the first day, and using either movement model we identify this periods as one of intensive localized movement. Fish 9603 was a member of a school that preyed on sand lance, and our analysis finds that the track is mostly localized motion. Although the track is short, our analysis finds that fish

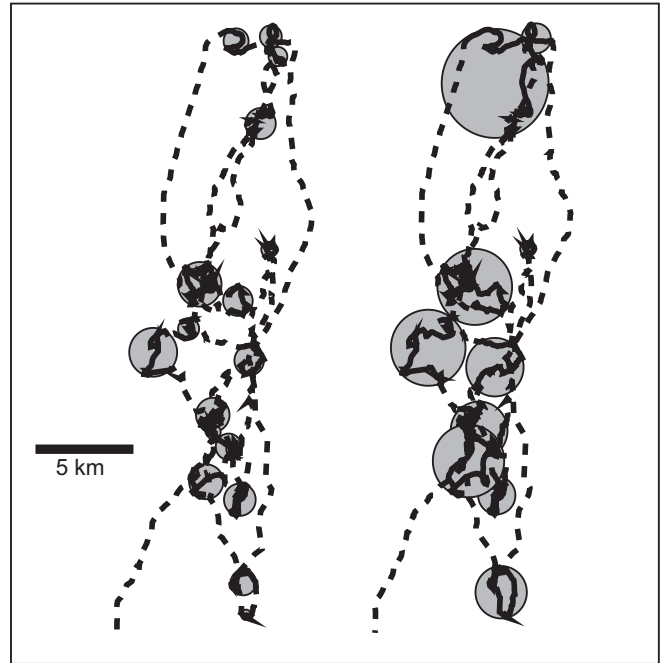


Fig. 6. Segmented bluefin tuna track with non-obvious separation between localized and long-ranged movement. This tuna was moving north and south in the Great South Channel. As in Fig. 5, identified localized motion is shown by solid lines and long-ranged motion by dashed lines. Left copy: biased turning model. Right copy: biased speed model.

9704 was in localized motion during the tracking period, and it was recorded to be foraging at the surface with its school. In all these cases, our algorithm successfully identified the observed feeding events as localized motion.

Not all the localized segments suggested by our algorithm correspond to observed feeding times. Some localized segments occur at night, when it was difficult or impossible to visually identify tuna behavior. Other localized segments may correspond to other forms of resource exploitation, perhaps lingering near a likely, but unoccupied, prey location or near a favorable thermal feature. These comparisons suggest that many of the localized segments identified by our algorithm do indeed correspond to resource exploitation, and that our algorithm performs best with finely sampled data.

4.4. Related work on tuna movement and distribution

Our data on Atlantic bluefin tuna comes from a study that has been described before in the literature, but not analysed previously for local versus long-range movement. Lutcavage et al. (2000) summarized and described the tracking effort, showing relationship of tracks to bathymetry in the Gulf of Maine, and verbally indicated times at which foraging behavior was observed. Some initial ideas about how tracks could be analysed as correlated and biased random walks (CRW and BRW) and how such work could lead to estimates of local population densities

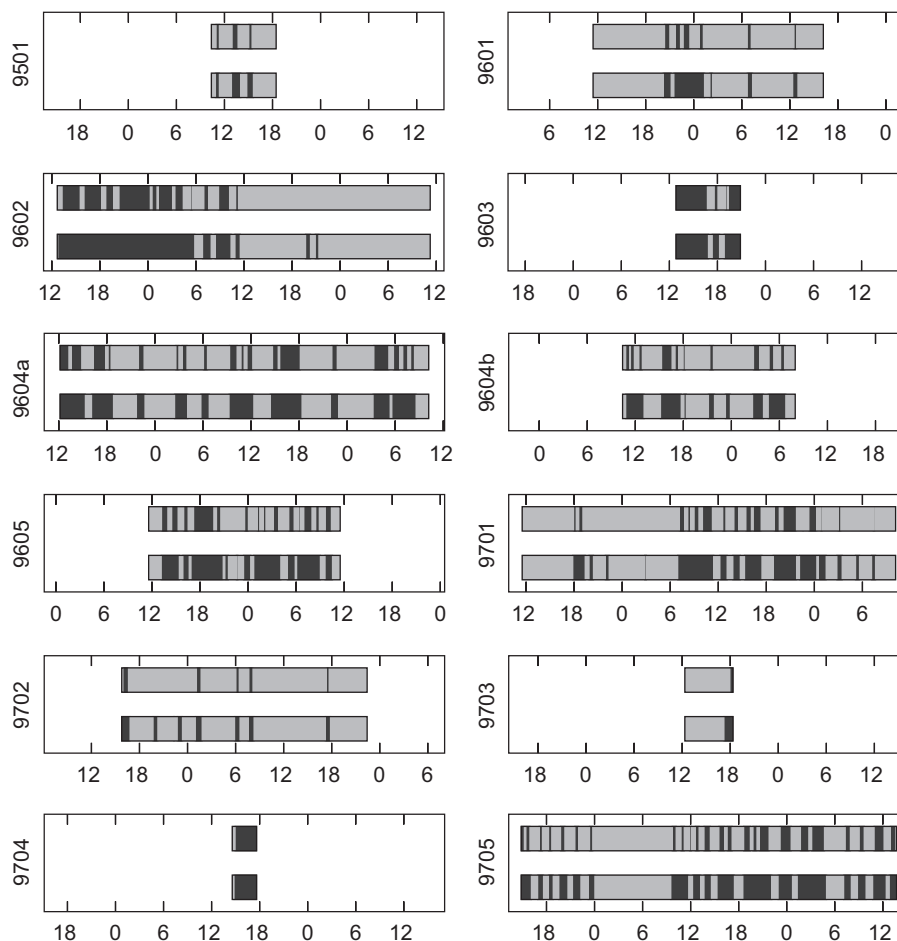


Fig. 7. Track segmentations as a function of time. Plotted are the movement type classifications for each track in our sample over the duration of motion (in hours past midnight local time). In each plot, the segmentation from the biased turning model (upper band) and the biased speed model (lower band) are shown. Dark bands corresponds to localized motion and light bands to long-ranged motion.

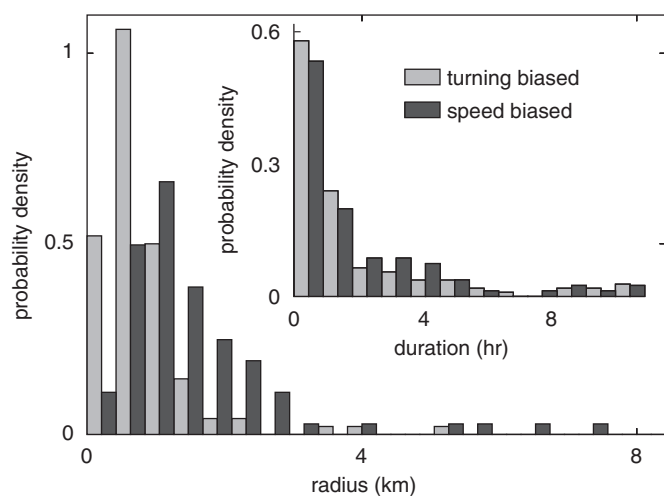


Fig. 8. Distributions of patch radii (km) and times (h) spent in long-ranged motion. The main chart shows histograms of the inferred patch radii at the optimal segmentation parameters for both movement models. The biased turning model suggests smaller patches than the biased speed model. The inset shows the distribution of durations of long-ranged segments. Both movement models lead to duration distributions with long tails and a mean of 2 h.

were formulated in [Newlands and Lutcavage \(2001\)](#). (See also, [Newlands](#), PhD thesis, University of British Columbia.) Finally, in [Newlands et al. \(2004\)](#), spectral methods were applied to identify distinct movement modes in which the “frequency in the rate of change of speed and turning angle” were strongly versus weakly correlated. It is well known that a high rate of turning, coupled to slow speed leads to a so-called “intensive search” strategy, leading to suggested interpretation of such correlations in terms of behavioral strategies. However, in our current work, we have used simpler geometric properties of track length and net displacement (coupled with an objective criterion) to identify local versus long-ranged movement, by passing the advanced spectral methods. We further use the segmentation of tracks and the statistical properties of switching between movement types to infer ecological aspects of interaction with the environment (putative resource sites), an aspect not previously considered in the work described above.

[Schick et al. \(2004\)](#) conducted an aerial survey of bluefin tuna schools in the Gulf of Maine, and [Royer et al. \(2004\)](#) similarly studied tuna schools in the Mediterranean Sea.

In contrast to our work, neither paper considers small scale individual movement of the fish nor track data of the type we consider. Similar to our tracks, Brill et al. (2002) used ultrasonic tags to track five juvenile tuna near the eastern shore of Virginia. The smaller number of individuals tracked, however, would limit the power of our methods. In all these cases, the distributions of tuna schools were related to oceanic features such as sea surface temperature, chlorophyll, thermal fronts, bathymetry, and water color fronts, etc. This work is complementary to ours in identifying the relationship of tuna to its environment. For example, Royer et al. (2004) used statistical techniques to check for spatial clustering and for association between the school distribution and the environmental variables. Since environmental variables did not explain all features of the distributions, the authors suggested that foraging, and inter- and intra-specific interactions were likely to influence these spatial distributions.

Block et al. (2005) describe an extensive electronic satellite tagging project involving nearly 800 Atlantic bluefin tuna migrating between the west Atlantic and the Mediterranean over a period of many months. The project involved larger distances and less detailed individual trajectories, with the main aim to determine hot-spots for possible spawning. This work, too, is less concerned with the small scale movement patterns of individuals (as in our paper) and more focused on trans-Atlantic migration and spawning hot-spots. Similarly Wilson et al. (2005) used satellite tags and Kalman filtering to track approximately 60 tuna in the northwestern Atlantic, focusing on the relationship between movement and sea surface temperature.

4.5. Related work on marine mammals

The work of Bailey and Thompson (2006) on dolphin foraging is most closely related to ours by ultimate goal, but not by detailed methodology. Using visual sighting of dolphins from a land-based instrument (theodolite) at Inverness Firth, Scotland, the authors analysed about 30 tracks for intensive and extensive search behavior, and compared with observed foraging. Classification of track portions into correlated (CRW) and biased (BRW) random walks were based on net-squared displacement, move length and turning angle distributions, and visual comparisons of bootstrap simulations and theoretical predictions (for CRW, by Kareiva and Shigesada, 1983, and for BRW, by Marsh and Jones, 1988). The authors applied a first-passage time analysis (Fauchald and Tveraa, 2003) to determine the spatial scale of dolphin activity. They identified sites of intensive searching and characterized the sizes of such sites (analogous to our “patches”). The conclusion that movement patterns can be distinguished between “extensive” and “intensive” searching is similar to our finding of local versus long-ranged movement pattern.

4.6. Related work on animal movement

Our investigation of movement models for bluefin tuna connects to a long tradition of work on biased or correlated random walks in organisms. (See Kareiva and Shigesada, 1983; Turchin, 1991; Casas and Aluja, 1997; Morales and Ellner, 2002, among many others.) Here we found that, for bluefin tuna, a combination of correlated biased random walks (of minimally two types) is needed to account for the motion. Unlike Kareiva and Shigesada (1983) and Root and Kareiva (1984), we did not find a linear relationship for net squared displacement, $D^2(t)$ versus t . (A similar deviation from this random walk model was noted by Ward and Saltz, 1994.) Our analysis is purely a Lagrangian one, and we do not attempt to infer population parameters such as rates of diffusion or transport from the limited data studied. (But see, e.g. Grünbaum, 1994; Hill and Häder, 1997; Grünbaum, 1998, 1999 for examples of the latter approach.)

While we investigated trajectories (i.e. time-records of motion), static animal tracks have been studied, e.g. by Ward and Saltz (1994) for dorcas gazelles in sands and by Becker et al. (1998) for wolves and game animals in snow. For example, Ward and Saltz (1994) found that gazelles made small displacements while foraging on lilies, interspersed by a few larger displacements to move to new foraging sites. The resolution of local versus long-ranged behavior connects their work to ours, but they could identify resource patches ab initio, unlike us. Other large-scale tracking of moving animals include satellite-tracked radio collared migrating caribou (Bergman et al., 2000). By comparing individual tracks to correlated random walks, the authors found evidence for a tendency to stay in or return to specific favored locations (site fidelity). This is similar to the localized motions we have described.

Terrestrial tracking studies have somewhat different goals and challenges, but as they are related, we comment briefly on some examples. In many of these, the topography, landscape features, and other environmental variables are a priori known, relatively static, and/or more easily quantified, so that animal behavior can be modeled in relation to its environment more directly. In an extensive land-based tracking effort (the Starkey project Preisler et al., 2004; Brillinger et al., 2002, 2004), the movements of hundreds of elk are modeled using stochastic differential equations, with potential functions representing landscape features. The authors make up the potential function by assuming repulsion from certain known features (such as roads) and attraction to others (e.g. grasslands). They use the data to produce vector fields of elk movement over the landscape, and to test the correlation between the movements and landscape features.

A marine environment presents special challenges, partly due to its inherent continual variability. Specific features that attract marine organisms, or that provide local (Girard et al., 2004) or long-ranged (Brillinger and Stewart, 1998) environmental cues are not easy to observe in real

time. (The former focused on man-made “patches”, whereas the latter argued that the motion of elephant seals, along a great circle in the north Pacific, is consistent with global navigation.) Other studies of fish movement such as Skalski and Gilliam (2000), Sparrevojn et al. (2002); Westerberg (1982) e.g., for spawning migration of ultrasonic-transmitter tagged Atlantic Salmon, are less concerned with modeling the movement of individuals and more with population dispersal.

4.7. Comparison with similar methods

In preliminary exploration of the data, we examined plots of track length $L(t)$, mean squared displacement $D^2(t)$, and tortuosity. We also examined speed, turning angles, heading angles, and correlations between them. These tests failed to uncover any identifiable trends. We further quantified the density of observed positions to test whether favored locations could be so identified, but such tests of the purely spatial information were also inconclusive. We also evaluated Marsh and Jones’ (1988) test for oriented movement based on the difference between heading and turn angle distributions. Applying this test to our tracks over short time windows, however, rarely yielded statistically significant results, which precluded us from drawing meaningful conclusions. The above exploratory analyses, though commonly used in the literature, failed to reveal striking patterns in our data. More interesting trends are seen in net displacement and track length, and this motivated our approach.

Girard et al. (2004) also compare displacement and track length for tuna, but for interactions with “artificial patches”, i.e., fish aggregating devices (FADs) of known location and size. They measure displacement and length of track with respect to a given FAD. Interestingly, they note that Marsac and Cayré (1998) find the “interaction radius” of a yellowfin tuna with a FAD to be about 1.8 km, similar to the mean radius we find for patches of localized movement for bluefin tuna. This agreement may suggest that the range at which tuna can perceive resources is approximately 1 km.

Fauchald and Tveraa (2003) suggest another method for estimating a typical patch size from track data. They consider the time required to cross a circle of given radius centered about each data point and take the radius that maximizes the variance of these times to be the typical patch size. Applying their analysis to our data yields a patch radius of about 10 km, substantially larger than the median radius we find. This disparity may be due to differences in the time scales of behavioral changes considered by the two models. By restricting our calculations of $\Delta D/\Delta L$ to a short window, our analysis allows us to identify distinct patches within a track. Fauchald and Tveraa’s method, on the other hand, averages over the entire track, so that several of the patches revealed by our analysis may be subsumed in each of their patches.

Unlike our relatively accurate track data, remote sensing technologies (including archival tagging) generate data that is sampled coarsely in space and time, typically less than 10 points per day. Moreover, the position of the tracked individual is usually not obtained directly: for example, it is to be inferred from light intensity recorded by sensors on moving fish. This means that the measurement process has significantly greater error than in our data. A variety of state-space models (SSM) based on a Bayesian approach have been developed for estimating measurement and process noise, for combining movement data with prior information, and for statistical testing of hypotheses (Jonsen et al., 2003).

For example, Morales et al. (2004) analysed elk data using a Bayesian approach. The low sampling rate of their data (once per day over 100 days) imply that correlations between steps are small in their model. To overcome these small correlations, they adopted the Bayesian approach so as to analyse many possible parameter sets consistent with the data. Our higher resolution data allows us to identify a set of best-fitting parameters for each movement model.

For comparison, we analysed our tracks using the “double-switch” model found in Morales et al. (2004) and WinBUGS 1.4 (Spiegelhalter et al., 1999). The resulting time series of movement states for each track was smoothed over a time window of $\Delta t = 43$ min to yield the final segmentations. Fig. 9 shows segmentations using this method for two tracks in our sample. Comparing with Figs. 5 and 6 shows that the Bayesian method yields

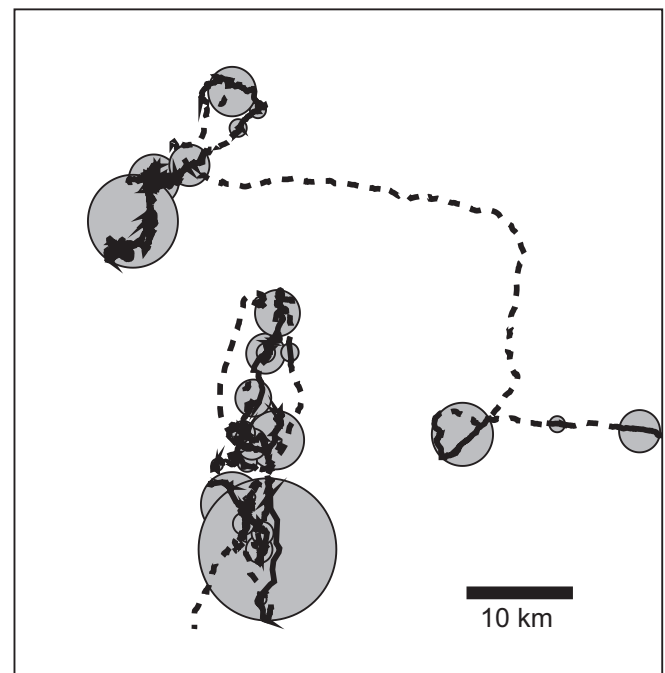


Fig. 9. An example of Bayesian analysis of our tracks. Segmentations based on a two-mode Bayesian analysis are shown for the tracks seen in Figs. 5 and 6. The Bayesian segmentations are qualitatively similar to those found by our method, but localized patches are larger and more frequent.

qualitatively similar segmentations, but that it classifies some relatively straight sections as localized and, in general, yields larger patches than our method.

The paper by Sibert et al. (2003) contains an excellent description of the application of the Kalman filter method to archival tagging data in bigeye and bluefin tuna (see also Sibert et al., 2006). A Kalman filter is similar to a predictor–corrector iteration wherein positions at previous times, together with an underlying assumed movement model and estimates of error in measurements are used to obtain the most probable current location for time series data. The method is based on a state-transition equation (the underlying movement model), an equation that describes measurement noise, and iterated updates of the estimates. Optimization of a log-likelihood function then leads to best fit parameters. In their approach, the Kalman filter estimates both the corrected locations of individuals as well as the parameters of advection–diffusion models (which are well known to be continuous extensions of biased random walks, see e.g. Okubo, 1980). In this sense, the Kalman filter is based on an Eulerian continuum modeling approach. The advantage of the technique is that it provides an estimate for the errors of measurement, as well as variance in parameter estimates.

Royer et al. (2005) provide a contrasting approach that combines a second superb review of state-space methods and current methods of tagging bluefin tuna, with clear descriptions of their distinct probabilistic Lagrangian (particle based) approach for modeling and data fitting. The authors show how environmental variables such as sea surface temperature can be assimilated to correlate interactions of tuna with its environment. They carefully explain and show tests of their Monte Carlo Particle Filter technique and compare it to performance of the Kalman filter using artificial data.

The ability to extract behavioral information from track data depends on the resolution of that data relative to time and spatial scales of interest. Codling and Hill (2005) showed how the sampling rate of trajectories can influence derived quantities such as mean speeds, turning angles, etc. In our data, the sampling rate is generally high enough (order of 1 min) to allow reasonable results for behaviors on the order of the foraging behaviors studied here. At the same time, other data sets allow for far greater level of detail. Brillinger et al. (2004, 2002) could reconstruct fuller spatial density contours, vector fields of apparent velocities at peak activity times, etc., as well as circadian cycles in activity. Their work was less concerned with relating the motion of the animals to specific behavior such as foraging. By comparison, our data allowed us to draw reasonable conclusions about individual behavior, but did not suffice for the level of resolution of space utilization that their data set could afford.

4.8. Other applications of the segmentation algorithm

Our algorithm can be generalized. Total length of track and displacement easily generalize from 2D to 3D, but

turning angles present certain complications in 3D. It can also be adapted to analyzing static records. Where the associated time record is unavailable, the window in the segmentation algorithm could be based on an arc length of track, rather than a time interval of motion. In this case, we could still classify long-ranged and localized portions and estimate the typical patch size associated with foraging, but we could not address how often patches are encountered. Our data were best fit by two motion types, but other situations or other organisms may require more. For example, many organisms have a “resting” state where motion has essentially ceased, or distinct predator avoidance behaviors, requiring a greater repertoire of movement types. Additionally, ocean currents can strongly affect tracks of marine organisms (Gaspar et al., 2006); removing the complicating effect of currents might enhance our ability to distinguish movement types.

Aside from the analysis of bluefin tuna, we carried out a number of preliminary tests of our segmentation algorithm using two motion types on data sets for other taxa. Our main motivation for this comparative study was to assess to what extent methods of this paper and lessons learned here could be generalized to other tracking studies. Identifying appropriate species and studies, obtaining data, and assessing the utility of the techniques on that data was a significant undertaking, and, in hind-sight, helped us to place our efforts into a wider context, despite limited payoff. Data were provided only for preliminary assessment purposes, so results can be only briefly summarized here.

Results for four elk tracks made available by Morales et al. (2004) appear reasonable, but the data are currently too limited to reliably estimate patch sizes. In tests with penguin data provided by Dee Boersma (Biology, University of Washington) our algorithm found few localized movement segments. When applied to data on albatross, kindly provided by Richard Phillips (British Antarctic Survey), our algorithm identifies distinct periods of long-ranged and localized motion, but since the data are sampled intermittently, technical aspects of interpolation need to be addressed before full interpretation. Uniquely, in caribou data provided by Robert Otto (Environment & Conservation, Newfoundland and Labrador) distinct regions of high and low $\Delta D/\Delta L$ were not found, possibly because of a low sampling rate. (See Codling and Hill, 2005 and previous comments for the effect of sampling rate.) Overall, while the segmentation algorithm described here likely has wider applicability, it is best suited to accurate track data sampled relatively finely and with relatively constant time step. Combining our method with more advanced filtering techniques may help to improve such results.

5. Conclusions

Our goal in this paper was to use observed movements of bluefin tuna to draw inferences about the difficult to observe distribution of resources they utilize. To do so, we

segmented tracks into long-ranged and localized movement patterns based on the ratio of displacement to length of track over a time window, using objective minimization criteria. We hypothesize that these segments are periods of time in which bluefin tuna migrate over long distances versus explore local resource patches, and thus we derive rough bounds on the distribution of resources exploited by bluefin tuna in the Gulf of Maine. We tested our method using two movement models, and found that the details of the inferred resource distribution are sensitive to the choice of model. Comparison between inferred localized movement and observed feeding activity suggests that our algorithm can effectively identify resource exploitation, although low sampling rates may hinder such inferences. We place an upper bound on the number density of resource patches in the Gulf of Maine of between 5 and 9 patches per 100 km² and estimate that the patches average about 1 km in size.

Our conclusions on bluefin tuna behavior and on their environment are limited by scarcity of data and accuracy of the movement models. For example, our estimates for ρ , the density of patches per unit area, should be considered as loose upper bounds, since we assumed that encounters with resource patches are random. Real bluefin tuna likely follow environmental cues such as topographic features, ocean fronts, and prey density to locate resources more efficiently, and resources may be clustered. Programs to track tuna are ongoing, and including more data would improve our ability to refine movement models and to test more detailed behavioral hypotheses. Ideally, physiological variables, such as hunger, and environmental variables, such as temperature and bathymetry, would be included in the movement model (e.g. Kirby, 2001). Further work could also consider depth information and schooling effects that we have neglected. It is to be hoped that future synergy between data collection and theoretical analysis will lead to a fuller understanding of tuna behavior and predictive models to aid in conservation efforts.

Acknowledgments

RG is supported by a National Science Foundation (USA) IGERT grant administered by Cornell University. ML is funded by National Marine Fisheries Service (Grant NA 06 FM 0460). NN and LEK were funded by the Natural Sciences and Engineering Research Council (Canada). We are grateful to the following: Richard Brill for tuna tracking; Ben Galuardi for mapping; Daniel Grünbaum, Harry Joe, and Juan Morales for advice; Richard Phillips (albatross), Robert Otto (caribou), Juan Morales (elk), and Dee Boersma (penguins) for sharing data. Finally, we thank our anonymous reviewers for insightful comments.

Appendix A. Numerical evaluation of heading and turn angle distributions

Here we develop an iterative method for calculating the heading and turn angle distributions for the biased turning

model. This procedure is used to find the steady-state distributions that we fit to the observed distributions.

Let \mathbf{H}_i denote the heading probability distribution after i moves, such that $\mathbf{H}_i(\theta)d\theta$ is the probability that the heading angle lies between θ and $\theta + d\theta$. In the first step of the vectorial bias movement model, we apply a turn, η , drawn from some distribution. This yields the intermediate heading vector \vec{u} shown in Fig. 4. We call the distribution of these intermediate headings $\mathbf{H}_{i+1/2}(\theta_{i+1/2})$. In our application to tuna, the turn distribution is a circular Laplace, denoted by $\mathbf{L}(\eta)$. The probability density of making a turn from θ_i to $\theta_{i+1/2}$ is $\mathbf{L}(\theta_{i+1/2} - \theta_i)$. Taking the integral of this density over all initial heading angles, weighted by the probability of being at that initial heading angle, yields

$$\mathbf{H}_{i+1/2}(\theta_{i+1/2}) = \int_{-\pi}^{\pi} \mathbf{H}_i(\theta_i) \mathbf{L}(\theta_{i+1/2} - \theta_i) d\theta_i. \quad (\text{A.1})$$

In all our integral evaluations, we approximate the heading distributions by fifth order splines with 50 knots over the interval $(-\pi, \pi)$.

Next we add in the bias vector, $b_\theta \vec{p}$. Some trigonometry shows that the heading after the bias is applied, θ_{i+1} , is related to the intermediate heading, $\theta_{i+1/2}$, by

$$\tan(\theta_{i+1}) = \frac{\sin \theta_{i+1/2} + b_\theta \sin \theta_p}{\cos \theta_{i+1/2} + b_\theta \cos \theta_p} \equiv \tan(\beta(\theta_{i+1/2})), \quad (\text{A.2})$$

where b_θ is the bias weight, and θ_p is the preferred heading. Since the function β is one-to-one over $(-\pi, \pi)$ we have

$$\mathbf{H}_{i+1}(\theta_{i+1}) = \frac{\mathbf{H}_{i+1/2}(\theta_{i+1/2})}{|\beta'(\theta_{i+1/2})|}, \quad (\text{A.3})$$

where β' is the derivative of $\beta(\theta_{i+1/2})$ with respect to $\theta_{i+1/2}$.

Starting from an initial heading distribution uniform over $(-\pi, \pi)$ (representing an unoriented animal), we iterate Eqs. (A.1) and (A.3) to converge to a steady-state heading distribution, \mathbf{H}_∞ . Our convergence criterion is that the root-mean-squared difference between \mathbf{H}_{i+1} and \mathbf{H}_i be less than 10^{-4} . Achieving this takes about 12 iterations for typical values of a and b_θ .

Once we have the steady-state heading distribution, $\mathbf{H}_\infty(\theta)$, we can use it to find the steady-state turn angle distribution. For any given heading, θ_i , the distribution of headings on the next step, $\mathbf{H}_{i+1}(\theta_{i+1}|\theta_i)$, can be found from Eqs. (A.1) and (A.3). Since the probability of making a turn angle ϕ is the probability of turning from θ_i to $\theta_{i+1} = \theta_i + \phi$, the distribution of turn angles given a previous heading of θ_i is $\Phi_i(\phi|\theta_i) = \mathbf{H}_{i+1}(\theta_i + \phi|\theta_i)$. To find the overall turn distribution we take the weighted integral over all possible steady-state initial headings:

$$\begin{aligned} \Phi_\infty(\phi) &= \int_{-\pi}^{\pi} \Phi_\infty(\phi|\theta) \mathbf{H}_\infty(\theta) d\theta \\ &= \int_{-\pi}^{\pi} \mathbf{H}_\infty(\phi + \theta|\theta) \mathbf{H}_\infty(\theta) d\theta. \end{aligned} \quad (\text{A.4})$$

Again we work with fifth order splines with 50 knots over $(-\pi, \pi)$. These splines are what we use to calculate

likelihoods for fitting a and b_θ to the observed distributions.

Appendix B. Supplementary data

Supplementary data associated with this article can be found in the online version at [10.1016/j.jtbi.2006.10.014](https://doi.org/10.1016/j.jtbi.2006.10.014).

References

- Bailey, H., Thompson, P., 2006. Quantitative analysis of bottlenose dolphin movement patterns and their relationship with foraging. *J. Anim. Ecol.* 75, 456–465.
- Becker, E., Spindler, M., Osborne, T., 1998. A population estimator based on network sampling of tracks in the snow. *J. Wildlife Manage.* 62, 968–997.
- Benhamou, S., Bovet, P., 1992. Distinguishing between elementary orientation mechanism by means of path analysis. *Anim. Behav.* 43, 371–377.
- Bergman, C., Schaefer, J., Luttich, S., 2000. Caribou movement as a correlated random walk. *Oecologia* 123, 364–374.
- Block, B.A., Teo, S.L.H., Walli, A., Boustany, A., Stokesbury, M.J.W., Farwell, C.J., Weng, K.C., Dewar, H., Williams, T.D., 2005. Electronic tagging and population structure of Atlantic bluefin tuna. *Nature* 434, 1121–1127.
- Brill, R., Lutcavage, M., Metzger, G., Stallings, J., Bushnell, P., Arendt, M., Lucy, J., Watson, C., Foley, D., 2002. Horizontal and vertical movements of juvenile North Atlantic bluefin tuna (*Thunnus thynnus*) in the western North Atlantic determined using ultrasonic telemetry, with reference to population assessment by aerial surveys. *Fish. Bull.* 100, 155–167.
- Brillinger, D., Stewart, B., 1998. Elephant-seal movements: modelling migration. *Can. J. Stat.* 26, 431–443.
- Brillinger, D., Preisler, H., Ager, A., Kie, J., Stewart, B., 2002. Employing stochastic differential equations to model wildlife motion. *Bull. Braz. Math. Soc., New Ser.* 33, 385–408.
- Brillinger, D., Preisler, H., Ager, A., Kie, J., 2004. An exploratory data analysis (EDA) of the paths of moving animals. *J. Stat. Plan. Infer., New Ser.* 122, 43–63.
- Casas, J., Aluja, M., 1997. The geometry of search movements of insects in plant canopies. *Behav. Ecol.* 8, 37–45.
- Chase, B.C., 2002. Differences in the diet of Atlantic bluefin tuna (*Thunnus thynnus*) at five seasonal feeding grounds on the New England continental shelf. *Fish. Bull.* 100, 168–180.
- Chatfield, C., 2001. *Time-series Forecasting*. Chapman & Hall, New York.
- Codling, E., Hill, N., 2005. Sampling rate effects on measurement of correlated and biased random walks. *J. Theor. Biol.* 233, 573–588.
- Fauchald, P., Tveraa, T., 2003. Using first-passage time in the analysis of area-restricted search and habitat selection. *Ecology* 84, 282–288.
- Gaspar, P., Georges, J.-Y., Fossette, S., Lenoble, A., Ferraroli, S., Maho, Y.L., 2006. Marine animal behaviour: neglecting ocean currents can lead us up the wrong track. *Proc. R. Soc. B*, E-print.
- Girard, C., Benhamou, S., Dagorn, L., 2004. FAD: fish aggregating device or fish attracting device? A new analysis of yellowfin tuna movements around floating objects. *Anim. Behav.* 67, 319–326.
- Grünbaum, D., 1994. Translating stochastic density-dependent individual behaviour with sensory constraints to an Eulerian model of animal swarming. *J. Math. Biol.* 33, 139–161.
- Grünbaum, D., 1998. Using spatially explicit models to characterize foraging performance in heterogeneous landscapes. *Am. Nat.* 151, 97–115.
- Grünbaum, D., 1999. Advection–diffusion equations for generalized tactic searching behaviours. *J. Math. Biol.* 38, 169–194.
- Hill, N., Häder, D., 1997. A biased random walk model for the trajectories of swimming microorganisms. *J. Theor. Biol.* 186, 503–526.
- Jammalamadaka, S.R., Kozubowski, T.J., 2004. New families of wrapped distributions for modeling skew circular data. *Commun. Stat. A—Theory and Methods* 33, 2059–2074.
- Jonsen, I.D., Myers, R.A., Flemming, J.M., 2003. Meta-analysis of animal movement using state-space models. *Ecology* 84, 3055–3063.
- Kareiva, P., Shigesada, N., 1983. Analyzing insect movement as a correlated random walk. *Oecologia* 56, 234–238.
- Kirby, D.S., 2001. On the integrated study of tuna behaviour and spatial dynamics: tagging and modelling as complementary tools. In: Sibert, J.R., Nielsen, J. (Eds.), *Electronic Tagging and Tracking in Marine Fisheries*. Kluwer Academic Publishers, The Netherlands, pp. 407–420.
- Lutcavage, M.E., Brill, R.W., Skomal, G.B., Chase, B.C., Goldstein, J.L., Tutein, J., 2000. Tracking adult North Atlantic bluefin tuna (*Thunnus thynnus*) in the northwestern Atlantic using ultrasonic telemetry. *Mar. Biol.* 137, 347–458.
- Marsac, F., Cayré, P., 1998. Telemetry applied to behaviour analysis of yellowfin tuna (*Thunnus albacares*) movements in a network of fish aggregating devices. *Hydrobiologia* 371/372, 155–171.
- Marsh, L.M., Jones, R.E., 1988. The form and consequences of random walk movement models. *J. Theor. Biol.* 133, 113–131.
- Morales, J.M., Ellner, S.P., 2002. Scaling up animal movement in heterogeneous landscapes: the importance of behavior. *Ecology* 83, 2240–2247.
- Morales, J.M., Haydon, D.T., Frair, J., Holsinger, K.E., Fryxell, J.M., 2004. Extracting more out of relocation data: building movement models as mixtures of random walks. *Ecology* 85, 2436–2445.
- Newlands, N.K., Lutcavage, M., 2001. From individuals to local population densities: North Atlantic bluefin tuna (*Thunnus thynnus*). In: Sibert, J.R., Nielsen, J. (Eds.), *Electronic Tagging and Tracking in Marine Fisheries*. Kluwer Academic Publishers, The Netherlands, pp. 421–441.
- Newlands, N.K., Lutcavage, M.E., Pitcher, T.J., 2004. Analysis of foraging movements of bluefin tuna (*Thunnus thynnus*). Individuals switch between two modes of search behavior. *Popul. Ecol.* 46, 39–53.
- Okubo, A., 1980. *Diffusion and Ecological Problems: Mathematical Models*. Springer, New York.
- Pauly, D., Christensen, V., Dalsgaard, J., Froese, R., Torres Jr., F., 1998. Fishing down marine food webs. *Science* 279, 860–863.
- Preisler, H.K., Ager, A.A., Johnson, B.K., Kie, J.G., 2004. Modeling animal movements using stochastic differential equations. *Environmetrics* 15, 643–647.
- Root, R.B., Kareiva, P., 1984. The search for resources by cabbage butterflies (*Pieris rapae*): ecological consequences and adaptive significance of Markovian movements in a patchy environment. *Ecology* 65, 147–165.
- Royer, F., Fromentin, J.M., Gaspar, P., 2004. Association between bluefin tuna schools and oceanic features in the western Mediterranean. *Mar. Ecol.-Prog. Ser.* 269, 249–263.
- Royer, F., Fromentin, J.M., Gaspar, P., 2005. A state-space model to derive bluefin tuna movement and habitat from archival tags. *Oikos* 109, 473–484.
- Schick, R.S., Goldstein, J., Lutcavage, M.E., 2004. Bluefin tuna (*Thunnus thynnus*) distribution in relation to sea surface temperature fronts in the Gulf of Maine (1994–1996). *Fish. Oceanog.* 13, 225–238.
- Sibert, J.R., Musyl, M.K., Brill, R.W., 2003. Horizontal movements of bigeye tuna (*Thunnus obesus*) near hawaii determined by Kalman filter analysis of archival tagging data. *Fish. Oceanog.* 12, 141–151.
- Sibert, J.R., Lutcavage, M.E., Nielsen, A., Brill, R.W., Wilson, S.G., 2006. Interannual variation in large scale movement of Atlantic bluefin tuna (*Thunnus thynnus*) determined from pop-up satellite archival tags. *Can. J. Fish. Aquat. Sci.* 63, 2154–2166.
- Skalski, G., Gilliam, J., 2000. Modeling diffusive spread in a heterogeneous population: a movement study with stream fish. *Ecology* 81, 1685–1700.
- Sparrevoorn, C., Nielsen, A., Støttrup, J.G., 2002. Diffusion of fish from a single release point. *Can. J. Fish. Aquat. Sci.* 59, 844–853.

- Spiegelhalter, D.J., Thomas, A., Best, N.G., 1999. WinBUGS version 1.2 user manual. MRC Biostatistics Unit, Cambridge, UK.
- Turchin, P., 1991. Translating foraging movements in heterogeneous environments into the spatial distribution of foragers. *Ecology* 72, 1253–1266.
- Ward, D., Saltz, D., 1994. Foraging at different spatial scales: dorcas gazelles foraging for lilies in the Negev Desert. *Ecology* 75, 48–58.
- Westerberg, H., 1982. Ultrasonic tracking of Atlantic salmon *Salmo-Salar* L. I. Movements in coastal regions. Institute of Freshwater Research, Drottningholm, Report 60, 81–101.
- Wilson, S.G., Lutcavage, M.E., Brill, R.W., Genovese, M.P., Cooper, A.B., Everly, A., 2005. Movements of bluefin tuna *Thunnus thynnus* in the northwestern Atlantic Ocean recorded by pop-up satellite archival tags. *Mar. Biol.* 146, 409–423.